Research Square

Preprints are preliminary reports that have not undergone peer review.
They should not be considered conclusive, used to inform clinical practice,
or referenced by the media as validated information.

Fe 3 O 4 , MnO 2 , and Na 2 S 2 O 8 amendments steer bacterial succession, fecal indicator regrowth, and humification during sewage sludge composting

Meihua Zhao
Guangzhou University
Zhiyu Cen
Guangzhou University
Zhen Yu
Dongguan University of Technology
Sirui Xu
Guangzhou University
François Nkinahamira
nkinahamis@gzhu.edu.cn
Guangzhou University

Research Article

Keywords: Sewage sludge composting, Bacterial succession, Fecal indicator regrowth, Humification, Redox amendments, Compost maturity

Posted Date: November 18th, 2026

DOI: https://doi.org/10.21203/rs.3.rs-11357721/v1

License: This work is licensed under a Creative Commons Attribution 4.0 International License.
Read Full License

Additional Declarations: No competing interests reported.

Abstract

Sewage sludge with a low carbon-to-nitrogen ratio often fails to reach the thermophilic phase that drives bacterial succession and pathogen reduction during composting. Redox-active amendments are added to intensify composting, but how each one reshapes the bacterial community, and with it fecal indicator regrowth and humification, has not been compared under identical conditions. Fe_3O_4, MnO_2, and $Na_2S_2O_8$ were each applied at 1% (w/w) to one dewatered sludge feedstock and compared with an unamended control over 42 days of reactor composting. Only $Na_2S_2O_8$ produced a thermophilic phase, peaking at 68°C and remaining at or above 55°C for four days, which meets the United States time–temperature condition for in-vessel sludge composting. It shifted the day-5 community toward Firmicutes (52.4%) and Actinobacteriota (16.5%), enriched the cellulose-degrading thermophile *Thermobifida* about 25-fold relative to the control, and prevented the early regrowth of *Escherichia–Shigella*, which reached 5.8 to 13.4% of the bacterial community in the other treatments. Fe_3O_4 and MnO_2 instead favored Proteobacteria and Bacteroidota, and Fe_3O_4 more than doubled the *Escherichia–Shigella* bloom relative to the control. All amendments raised humic acid and the humic-to-fulvic acid ratio relative to the control, yet total humic substances fell by 17 to 24% in every treatment, least under MnO_2 and $Na_2S_2O_8$. Ratio-based maturity indices therefore indicated progressive humification while humic carbon was being lost. Amendment choice determines which degrader and indicator populations develop, and maturity certification for land application should include an absolute humic measure.

1. Introduction

Municipal sewage sludge is one of the fastest-growing waste streams worldwide. Global production exceeds 53 million tons (dry basis) annually and continues to rise as wastewater treatment coverage expands (Feng et al. 2023), with China alone generating 13.62 million tons (dry basis) in 2022 (Liu et al. 2025; Zhao et al. 2026). Landfilling, incineration, and direct land application all face tightening environmental, economic, and regulatory constraints (Nkinahamira et al. 2019; Li et al. 2023; Liu et al. 2026). At the same time, sludge contains 30 to 60% organic matter, along with nitrogen, phosphorus, and potassium, making it a secondary resource rather than only a disposal burden (Balkrishna et al. 2024). Returning sludge to soil, however, requires a product that meets both stability and pathogen-reduction requirements, and land-application rules commonly require pathogen reduction (US EPA 1993).

Aerobic composting is among the most practical routes for converting sludge into a land-applicable product. Microbial degradation and stabilization transform unstable residues into humified material that improves soil structure and nutrient retention, with humic acid (HA) of particular interest for compost stability and agronomic value (Guo et al. 2019; Sun and Awasthi 2025; Tao et al. 2025). Two conditions govern whether that product can be applied to land. The first is humification, which in sludge is constrained by refractory lignocellulosic material that resists degradation and limits precursor release, as well as by fluctuating temperature, moisture, and oxygen availability (Lu et al. 2025; Tao et al. 2025). It also depends on the bacterial community, since thermophilic Firmicutes and Actinobacteriota hydrolyze lignocellulose and release humic precursors (Bui et al. 2023; Li et al. 2024). The second is pathogen

reduction, since sludge carries enteric bacteria and antibiotic-resistance determinants whose inactivation depends on sustained thermophilic exposure; a compost that matures without adequate self-heating therefore remains unsuitable for agricultural use (Balkrishna et al. 2024; Pan et al. 2024).

Amendments that modify redox conditions have been proposed to intensify both processes. Fe_3O_4 supports Fe^{2+}/Fe^{3+} cycling and electron transfer within composting systems (Chen et al. 2024); MnO_2 participates in multivalent $Mn^{2+}/Mn^{3+}/Mn^{4+}$ transformations that promote oxidative conversion of organic substrates across a broad pH range (Qi et al. 2021); and $Na_2S_2O_8$ can be thermally activated to generate sulfate radicals and other reactive oxygen species (ROS) (Xing et al. 2022). Because these materials differ substantially in redox chemistry, they may not act interchangeably, and the same dose could favor organic-matter breakdown, humic condensation, or thermal output to different degrees, and select different degrader and indicator populations. ROS concentration serves as a comparative index of oxidative intensity rather than a mechanistic endpoint (Wang et al. 2025).

Although each amendment has been reported to improve composting performance, studies have examined them independently, on different feedstocks, at different doses, and over different durations (Wang et al. 2021; Qi et al. 2024; Chen et al. 2024). When oxidative amendments were combined, the aim was to maximize aggregate performance rather than separate their individual contributions (Wang et al. 2026). None of these studies asked whether an amendment can supply the thermophilic phase that sludge with a low carbon-to-nitrogen ratio cannot reach on its own, judged against the time–temperature conditions that govern land application, how each amendment redirects bacterial succession, including thermophilic degraders and fecal indicators, or what these effects cost in the humic quality and elemental load of the recycled product. Without that evidence, operators cannot match an amendment to the compost's intended destination.

This study compares Fe_3O_4, MnO_2, and $Na_2S_2O_8$, each applied at 1% (w/w) to the same dewatered sewage sludge feedstock over a 42-day aerobic composting cycle, against an unamended control. We evaluate three outcome domains: bacterial succession, including thermophilic degraders and the fecal indicator *Escherichia–Shigella*; thermophilic behavior; and humic composition (humic and fulvic acid contents, degree of polymerization, and dissolved organic matter character). Organic-matter degradation, pH, electrical conductivity, and ·OH-equivalent ROS are reported as supporting process variables. The aim is to identify differences among the three amendments under identical conditions and translate those differences into guidance for returning sludge compost to land without transferring pathogens or unstable organic matter to the receiving soil.

2. Materials and Methods

2.1 Composting design and substrate characterization

Dewatered sewage sludge was used as the primary substrate, supplemented with rice straw and wheat bran. The sludge was obtained from a local municipal wastewater treatment plant, while rice straw and

wheat bran were collected from nearby agricultural sources. The raw materials were homogenized and mixed at a dry weight ratio of 6:5:1 (sludge: rice straw: wheat bran). The total organic carbon (TOC) contents of the sludge, rice straw, and wheat bran were 363.77, 463.32, and 513.18 g kg^{-1}, and their total nitrogen (TN) contents were 43.33, 14.76, and 25.21 g kg^{-1}, respectively, giving an initial C/N ratio of 13.96 for the composting mixture. All treatments used the same substrate composition, so that the three amendments were compared under identical initial conditions. Fe_3O_4 (≥ 99% purity, particle size < 0.15 mm), MnO_2 (≥ 99%) and $Na_2S_2O_8$ (≥ 99%) were purchased from Shanghai Macklin Biochemical Co., Ltd. (Shanghai, China) and used as received. A single dose of 1% of total dry weight was applied to each amendment, so that treatments differed only in amendment identity and not in loading. On an elemental basis, this dose corresponds to 7.2 g Fe (Fe_3O_4), 6.3 g Mn (MnO_2), or 1.9 g Na and 2.7 g S ($Na_2S_2O_8$) per kg of dry feedstock, which is the load each amendment adds to the recycled product.

The composting experiment was conducted in rectangular plastic reactors (50 cm × 40 cm × 30 cm; working volume 60 L) insulated with a 3 cm cotton layer to minimize heat loss. The initial moisture content was adjusted to 60%. Four treatments were established: (i) an unamended control (CK); (ii) Fe_3O_4 (1%, w/w); (iii) MnO_2 (1%, w/w); and (iv) $Na_2S_2O_8$ (1%, w/w). Each treatment was performed in triplicate and run for 42 days. Materials were manually turned every 3 days during the initial phase (days 0 to 12) and every 6 days thereafter to ensure adequate aeration. Pile temperature was recorded daily using a digital thermocouple center thermometer (Tuoerwei model T-105); reported values are the means of the three replicate reactors. Samples were collected by five-point sampling on days 0, 5, 11, 16, 22, 32, and 42 and were divided into a fresh portion, an air-dried and sieved (< 1 mm) portion for physicochemical and humus analyses, and a portion stored at − 80°C for DNA extraction.

2.2 Physicochemical analysis

Moisture content was determined by oven drying at 105°C to constant weight. The pH and electrical conductivity (EC) were measured in a 1:10 (w/v) compost-to-deionized water extract using a pH meter and a conductivity meter, respectively (Nkinahamira et al. 2019). OM content was determined by loss on ignition: dried samples were combusted at 600°C for 3 h in a muffle furnace, cooled to room temperature, and reweighed; OM was calculated from the mass lost on ignition (Paredes et al. 2000). OM degradation was expressed on an ash-free basis, treating ash as an inert tracer. Total nitrogen (TN) was measured by alkaline potassium persulfate digestion followed by UV spectrophotometry (Ministry of Environmental Protection of China 2012).

2.3 Reactive oxygen species determination

Reactive oxygen species (ROS) generated during composting were determined using the sodium benzoate trapping method coupled with high-performance liquid chromatography (HPLC; LC-16, Shimadzu, Japan) at 255 nm, following previously reported procedures (Ste-Marie et al. 1996). The detection limit was 0.1 μmol kg^{-1}. Because sodium benzoate primarily reacts with hydroxyl radicals (·OH) but may also capture other highly reactive oxidizing species generated during composting, particularly in the $Na_2S_2O_8$ treatment, the measured values are interpreted as ·OH-equivalent ROS concentrations. The

method was applied identically to all treatments, and the resulting concentrations are therefore used as a comparative index of oxidative intensity between amendments rather than as a mechanistic endpoint.

2.4 Humus fractionation

Humus fractions were separated by alkaline extraction and acid precipitation (Zhao et al. 2026). Briefly, 5.000 g of air-dried sample was extracted with 50 mL of 0.1 mol L^{-1} NaOH–0.1 mol L^{-1} $Na_4P_2O_7 \cdot 10H_2O$ at 25°C and 240 rpm for 24 h, followed by centrifugation and filtration through a 0.45 μm membrane to obtain the humic-substance (HS) extract. The extract was acidified to pH 1.0 using 6 mol L^{-1} HCl and allowed to stand for 12 h. After centrifugation, the supernatant was collected as fulvic acid (FA), while the precipitate was redissolved in 0.1 mol L^{-1} NaOH as HA. HS, HA, and FA were quantified as organic carbon using a TOC analyzer. Each fraction was quantified in a separate solution, namely the alkaline extract for HS, the redissolved acid precipitate for HA, and the acidified supernatant for FA. HS, HA, and FA are therefore reported as independently measured fractions rather than as a closed mass balance, since carbon is not fully recovered through the acid separation step. The degree of polymerization (DP) was calculated as the HA/FA ratio. These parameters indicated the degree of humification during sludge composting.

2.5 UV–Vis spectroscopy

UV–Vis spectra of the alkaline HS extract were recorded on a spectrophotometer (UH4150, Hitachi, Japan) over 200 to 400 nm in a 1 cm quartz cell. The indices $A_{260-280}$, E_{250}/E_{365}, and E_{253}/E_{203} were calculated to characterize aromaticity, molecular size, and structural evolution of the dissolved organic matter. $SUVA_{254}$ and $SUVA_{280}$ were calculated as the absorbance at 254 and 280 nm divided by the dissolved organic carbon concentration of the same solution and are expressed in L mg^{-1} m^{-1}.

2.6 Three-dimensional excitation–emission matrix fluorescence spectroscopy

Three-dimensional excitation–emission matrix (3D-EEM) fluorescence spectra were obtained using a fluorescence spectrophotometer (F-7000, Hitachi, Japan) with excitation wavelengths of 200–500 nm and emission wavelengths of 250–550 nm. Parallel factor analysis (PARAFAC) was conducted using MATLAB R2017a to identify the major fluorescent components and evaluate the transformation of dissolved organic matter during humification.

2.7 Microbial community analysis and pathogen indicators

Microbial community composition was determined by high-throughput sequencing of the bacterial 16S rRNA gene. DNA was extracted using the PowerSoil DNA Isolation Kit (QIAGEN), and the V4 region was amplified with primers 515F and 806R. Sequencing was performed on an Illumina NovaSeq 6000 by Magigene Biotechnology Co., Ltd. (Guangzhou, China). Raw reads were quality-filtered and resolved into amplicon sequence variants using QIIME2 with DADA2, and taxonomy was assigned against the SILVA 138 reference database. Pathogen indicators are reported as the relative abundance of the genus-level

Escherichia–Shigella group within the bacterial community. This sequence-based indicator of fecal contamination does not replace culture-based enumeration of viable pathogens.

2.8 Statistical analysis

All measurements were performed using three independent reactors (n = 3), and results are presented as mean ± standard deviation. Microsoft Excel 2017 was used for data organization, Origin 2022 for figure preparation, and MATLAB R2017a for EEM-PARAFAC analysis. Treatment effects on the humic-substance variables (HS, HA, FA, and DP) were tested by one-way analysis of variance (ANOVA) across the four treatments at each sampling time, followed by pairwise comparison of each amended treatment against CK. Probabilities from these three pairwise tests were Bonferroni-adjusted, and adjusted $p < 0.05$ was taken as significant. Pearson correlation analysis was performed using SPSS 22.0 to evaluate relationships among physicochemical properties, humus components, and microbial communities. For correlations between physicochemical properties and humus components, mean values from triplicate reactors at seven sampling points (days 0, 5, 11, 16, 22, 32, and 42) were used for each treatment (n = 7). For microbial correlation analyses, four sampling points (days 0, 5, 16, and 42) were included (n = 4). Correlation coefficients are reported with exact p-values based on n − 2 degrees of freedom, and associations not reaching $p < 0.05$ are described as trends. No multiple-comparison correction was applied, and because the correlations use sampling times as cases, they describe coordinated temporal variation rather than independent observations.

3. Results and Discussion

3.1 Thermal and physicochemical evolution

3.1.1 Temperature and thermophilic behavior

Temperature profiles (Fig. 1a) followed the characteristic heating, thermophilic, and cooling sequence but differed among treatments. CK and MnO_2 peaked at 44.2°C and 46.0°C on day 5, and Fe_3O_4 reached only 42.0°C over the same interval, so none of the three crossed the 50°C thermophilic threshold. $Na_2S_2O_8$, in contrast, rose to 68°C by day 2 and held above 50°C from day 1 to day 6, six consecutive days. It remained at or above 55°C from day 2 to day 5, which meets the United States condition for in-vessel composting of sewage sludge, at least 55°C for 3 days (US EPA 1993), and covers four of the six days specified in the Chinese technical guideline (Ministry of Housing and Urban-Rural Development 2011). None of the other treatments reached 55°C at any point, so none met either condition (Table 1). These durations were measured in 60 L reactors and indicate relative capacity rather than full-scale compliance. The subdued self-heating in CK, Fe_3O_4 and MnO_2 is consistent with the low initial C/N ratio of the substrate (13.96), well below the 25 to 30 range recommended for thermophilic composting (Puyuelo et al. 2011; Shen et al. 2024), since a carbon-limited, nitrogen-rich substrate restricts the respirable carbon needed to sustain a thermophilic phase (Hamoda et al. 1998). This constraint is characteristic of dewatered sewage sludge and represents a realistic, rather than idealized, composting

substrate. The capacity of $Na_2S_2O_8$ to overcome it is therefore the clearest single operational distinction among the four treatments, and it matters for pathogen reduction, which during composting depends on sustained thermophilic exposure (Section 3.3). By day 42, all treatments had converged to 30–33°C, indicating progression toward maturation.

Fe_3O_4 produced a secondary thermal event that no other treatment displayed. After cooling to 37.5°C by day 16, its temperature rose to 47.0 to 47.5°C between days 17 and 19, the highest values recorded in that treatment, before declining again. This late self-heating immediately preceded the day-22 maximum in HA described in Section 3.2, and indicates a delayed phase of substrate degradation rather than a uniformly gradual profile. In the $Na_2S_2O_8$ treatment, thermal activation of persulfate under the prevailing alkaline conditions provides a plausible additional heat source, since $S_2O_8^{2-}$ activation and the subsequent radical-mediated depolymerization both release energy and liberate soluble substrates for microbial respiration (Zhou et al. 2024).

3.1.2 pH, EC and nitrogen

The pH of all treatments rose from initial values of 7.1 to 7.8 to a peak of 8.5 to 8.9 within five days, consistent with protein deamination and urea hydrolysis during early decomposition (Fig. 1b). It then declined, with CK remaining highest and most stable (≈ 8.7 to 8.8), Fe_3O_4 and MnO_2 fell to ≈ 7.5 to 7.7 by day 42, and $Na_2S_2O_8$, which started lowest, declined most (≈ 7.3). The mildly alkaline early phase is relevant to the oxidative chemistry of the amendments, since it favors conversion of $SO_4^{\bullet-}$ to ·OH (Luo et al. 2026), whereas precipitation of Fe^{3+} and Mn^{4+} species above pH 9 may limit sustained radical generation in the metal-oxide treatments.

EC rose in all treatments and was consistently highest under $Na_2S_2O_8$ (Online Resource 1, Fig. S1a), from 2.24 to 3.00 mS cm^{-1}, compared with 1.56 to 1.98 mS cm^{-1} in CK, 1.25 to 2.06 mS cm^{-1} under Fe_3O_4 and 1.60 to 2.05 mS cm^{-1} under MnO_2. This reflects the sulfate-derived ionic load introduced with the amendment, along with soluble salts released during accelerated mineralization, and is relevant to salinity-sensitive end uses. EC increased with DP in all four treatments ($r = 0.47$ to 0.85, $n = 7$), becoming significant only under Fe_3O_4 ($r = 0.848$, $p = 0.016$). Total nitrogen concentration fell during the first 11 to 16 days and then rose (Online Resource 1, Fig. S1b), ending 10.72% above its initial value under $Na_2S_2O_8$ and 7.49% above in CK, while Fe_3O_4 and MnO_2 returned close to their starting concentrations. Because no nitrogen mass balance was performed and dry-mass loss was not accounted for, these are concentration dynamics only and cannot be read as net nitrogen retention. The C/N ratio fell in every treatment (Online Resource 1, Fig. S1c), most steeply under $Na_2S_2O_8$ (14.83 to 10.12) and least under MnO_2 (14.85 to 11.63).

3.1.3 Organic matter degradation and oxidative intensity

OM declined continuously in all treatments (Fig. 1c), from a common initial value of 75.0 to 75.6% to 56.6 to 60.7% by day 42. On an ash-free basis (Section 2.2), the degradation extents were 49.95 ± 2.77% (CK), 55.53 ± 1.21% (Fe_3O_4), 52.19 ± 0.49% (MnO_2) and 56.53 ± 0.42% ($Na_2S_2O_8$). The treatments differed overall (one-way ANOVA, $F = 11.6$, $p = 0.003$), but after Bonferroni correction, only $Na_2S_2O_8$ exceeded CK

significantly (+ 6.6 percentage points, p = 0.046); Fe_3O_4 was marginal (+ 5.6 points, p = 0.099) and MnO_2 did not differ from CK (+ 2.2 points, p = 0.72). Fe_3O_4 and MnO_2 therefore increased organic-matter degradation relative to CK without reaching thermophilic temperatures, indicating that the benefit of amendment is not contingent on thermophilic operation alone.

·OH-equivalent ROS followed a rise-and-fall pattern in every treatment, peaking on day 5 (Fig. 1d). Relative to CK (73.8 μmol kg^{-1}), peak concentrations reached 106.1 μmol kg^{-1} under Fe_3O_4 and 100.1 μmol kg^{-1} under MnO_2, while $Na_2S_2O_8$ reached 163.8 μmol kg^{-1}, 2.22-fold that of CK. Concentrations declined in all treatments after day 11, although $Na_2S_2O_8$ remained highest and showed a secondary shoulder of about 55–60 μmol kg^{-1} near day 16. Oxidative intensity therefore followed the order $Na_2S_2O_8$ > Fe_3O_4 ≈ MnO_2 > CK, was most pronounced early in composting, and matched the ordering of organic-matter degradation. As set out in Section 2.3, these values are a comparative index rather than absolute hydroxyl-radical concentrations, and the sulfate-radical contribution is expected to be substantial under $Na_2S_2O_8$ (Yang et al. 2020; Hong et al. 2024).

3.2 Humic composition

3.2.1 Humic acid, fulvic acid and degree of polymerization

HA, FA and the degree of polymerization (DP = HA/FA) describe the composition of the humic pool and its change during composting (Fig. 2). HA followed a non-monotonic trajectory in every treatment rather than increasing continuously. From a common initial value of 26.45 to 26.69 mg g^{-1}, HA rose sharply under $Na_2S_2O_8$ by day 5 (31.49 ± 0.21 mg g^{-1}) while CK and MnO_2 declined slightly over the same interval (25.19 ± 0.06 and 26.31 ± 0.64 mg g^{-1}), so the early accumulation coinciding with the day-5 ·OH-equivalent ROS maximum was specific to the persulfate treatment. HA then peaked at day 16 in CK (30.16 ± 0.80) and $Na_2S_2O_8$ (33.40 ± 0.30) and at day 22 in Fe_3O_4 (33.76 ± 0.39), the latter immediately following that treatment's day 17 to 19 thermal event (Section 3.1.1), before declining during maturation. By day 42, HA had settled at 27.22 ± 0.07, 29.06 ± 0.10, 29.38 ± 0.47, and 29.50 ± 0.30 mg g^{-1} in CK, Fe_3O_4, MnO_2, and $Na_2S_2O_8$. Day-42 differences were significant (one-way ANOVA, F = 41.6, p = 3.2×10^{-5}) and each amendment exceeded CK after Bonferroni correction (Fe_3O_4 +1.84 mg g^{-1}, p < 0.001; MnO_2 +2.16 mg g^{-1}, p = 0.004; $Na_2S_2O_8$ +2.28 mg g^{-1}, p < 0.001), as were differences at every sampling day from day 5 onwards (p ≤ 8.6×10^{-5}). The mid-composting maximum, followed by partial decline, indicates that the amendments accelerated HA formation rather than increasing its ultimate yield, and that the endpoint value alone understates the difference between treatments.

FA decreased continuously in all treatments, from an initial 41.91 mg g^{-1} to 22.06, 22.89, 22.75, and 22.24 mg g^{-1} in CK, Fe_3O_4, MnO_2, and $Na_2S_2O_8$ (F = 81.2, p = 2.5×10^{-6} at day 42). Rising HA against falling FA shifted the balance of the humic pool toward its more condensed fraction, and DP accordingly increased from 0.62 to 0.64 at day 0 to 1.23 ± 0.005 (CK), 1.27 ± 0.007 (Fe_3O_4), 1.29 ± 0.022 (MnO_2), and 1.33 ± 0.006 ($Na_2S_2O_8$). All amendments raised DP relative to CK (one-way ANOVA at day 42, F = 30.1, p

= 1.1 × 10^{-4}; Bonferroni-corrected pairwise p = 0.007, 0.035, and 0.0001), with the highest value occurring under $Na_2S_2O_8$, although the absolute margins are small at 0.04 to 0.09 DP units.

Total humic substances, however, declined in every treatment, from 71.0 to 72.2 mg g^{-1} at day 0 to 53.75 ± 0.02 (CK), 55.75 ± 0.10 (Fe_3O_4), 59.34 ± 0.91 (MnO_2) and 58.65 ± 0.02 mg g^{-1} ($Na_2S_2O_8$) by day 42, a net loss of 17 to 24%. The amended treatments retained significantly more HS than CK (F = 97.7, p = 1.2 × 10^{-6}; all three Bonferroni-corrected comparisons p ≤ 0.001), with MnO_2 and $Na_2S_2O_8$ retaining the most. Humification in this system therefore expressed itself as a change in the composition of the humic pool rather than as net accumulation: the condensed HA fraction gained at the expense of FA while the pool as a whole contracted, and the amendments acted as much by limiting the loss of humic carbon as by promoting its formation. This distinction matters for assessing compost maturity. DP, and the fluorescence and UV–Vis indices reported below, all improved while total humic carbon fell by roughly a fifth, so ratio-based humification indices can indicate progressive maturation in a system that is losing humic material. Where the quantity of humic substances in the final product is the objective, indices of this kind should be read alongside an absolute measurement. For a product destined for land, a maturity assessment based on such ratios alone would overstate the humic carbon actually returned to soil.

3.2.2 Fluorescent DOM components

EEM-PARAFAC resolved three fluorescent components (Fig. 3): a protein-like component (C1) with Ex/Em regions at 225 to 280/330 nm and 300 to 350/400 nm, a humic acid-like component (C2) at 230 to 255/410 nm, and a highly conjugated humic-like component (C3) centered near 475 nm (Xie et al. 2023; Lu et al. 2024). C1, associated with soluble microbial products and readily biodegradable substrates, declined in all treatments, whereas C2 and C3 increased throughout composting. The shift from protein-like toward humic-like fluorescence is consistent with progressive DOM humification and structural stabilization (Xie et al. 2023; Bang et al. 2024), and was most pronounced under $Na_2S_2O_8$.

Treatment-dependent differences were substantial (Online Resource 1, Fig. S2). Under $Na_2S_2O_8$, the relative Fmax contribution of C1 fell from 83.26% to 19.55% while C2 rose from 9.25% to 45.03% and C3 from 7.49% to 35.42%, a near-complete inversion of the initial DOM composition. Fe_3O_4 and MnO_2 also increased C2 and C3, though less markedly. The amendments therefore influenced not only the extent of DOM humification but also the relative balance of the two humic-like components, a distinction discussed in Section 3.4.

3.2.3 UV–Vis spectral indices

The UV–Vis indices (Online Resource 1, Fig. S3) were consistent with the humic-fraction and fluorescence results. $A_{260-280}$, $SUVA_{254}$, and $SUVA_{280}$ increased throughout composting, indicating progressive aromatic condensation, with the largest increases under $Na_2S_2O_8$. E_{250}/E_{365} decreased, consistent with increasing molecular size and complexity, and E_{253}/E_{203} increased in the amended treatments, particularly under $Na_2S_2O_8$, indicating greater aromatic substitution. Taken together with the

rise in DP, these changes indicate that the amendments promoted conversion of labile organic matter into more aromatic and condensed humic structures, consistent with the compositional shift described in Section 3.2.1.

3.3 Pathogen indicators and bacterial succession

3.3.1 Pathogen indicators

Escherichia–Shigella, the sequence-based fecal indicator, accounted for 0.14% of the bacterial community in the initial mixture. In the three treatments that stayed below 50°C, it then increased sharply, reaching 5.76% in CK, 6.03% under MnO_2, and 13.40% under Fe_3O_4 by day 5, whereas under $Na_2S_2O_8$ it remained at 0.10% (Fig. 4b; Online Resource 1, Table S2). $Na_2S_2O_8$ therefore prevented the early regrowth of this enteric indicator that occurred in every other treatment, a 58-fold difference from CK at day 5, while Fe_3O_4 more than doubled the regrowth relative to CK. The suppression coincided with the only thermophilic phase in the experiment (Section 3.1.1) and is consistent with the established role of elevated composting temperature in pathogen inactivation (Chen et al. 2023). The difference was transient. By day 16, the indicator had fallen below 1% in all treatments, and by day 42 it had returned to 0.08 to 0.14%, close to the initial mixture level, in every compost. The pathogen-reduction benefit of $Na_2S_2O_8$ therefore lies in the composting phase, when enteric-bacterial regrowth matters for handling and process compliance, rather than in a lower indicator level in the finished product. Because this genus is also a potential host of antibiotic-resistance genes (Pan et al. 2024), its early suppression remains relevant to land application. Sequencing was not replicated, and culture-based enumeration was not performed, so these values show the direction of the effect rather than a verified reduction in viable pathogens.

3.3.2 Phylum-level succession

The raw materials were dominated by Planctomycetota, Acidobacteriota, Bacteroidota and Proteobacteria, with Planctomycetota and Acidobacteriota together accounting for about 43% of relative abundance (Fig. 4a). As composting progressed, Bacteroidota, Proteobacteria, Firmicutes and Actinobacteriota became dominant in all treatments, and treatment-dependent differences emerged by day 5. $Na_2S_2O_8$ showed the highest abundances of Firmicutes (52.4%) and Actinobacteriota (16.5%), compared with 38.0% and 2.1% in CK, the eight-fold enrichment of Actinobacteriota being the sharper contrast. Firmicutes remained highest under $Na_2S_2O_8$ at day 16 (35.4%), and Actinobacteriota rose further by day 42 (21.8% against 9.8% in CK), so the thermophilic assemblage persisted well beyond the temperature maximum. This co-occurred with the thermophilic phase described in Section 3.1.1 and is consistent with the preference of Firmicutes for high-temperature conditions, where they contribute to rapid hydrolysis of organic substrates (Li et al. 2024; Lu et al. 2024), and with the recognized capacity of Actinobacteriota to degrade recalcitrant organic matter during later-stage stabilization (Bang et al. 2024).

Fe_3O_4 and MnO_2 instead promoted communities enriched in Proteobacteria and Bacteroidota. Fe_3O_4 developed a Proteobacteria-dominant community by day 5, while MnO_2 supported a more balanced Proteobacteria, Bacteroidota, and Firmicutes assemblage. Proteobacteria reached 53.2% under Fe_3O_4 and 36.2% under MnO_2 at day 5, compared with 29.7% in CK and only 14.1% under $Na_2S_2O_8$, the clearest distinction between the metal-oxide and persulfate communities. Because Proteobacteria and Bacteroidota are associated with using soluble organic compounds and lignocellulose-derived intermediates under mesophilic conditions (Xie et al. 2023), their enrichment likely reflects enhanced substrate turnover rather than thermophilic selection. By day 11, Bacteroidota dominated all amended treatments at about 40% of total abundance, and by day 42 community structures had become more even across treatments, reflecting progressive maturation.

3.3.3 Genus-level succession

At the genus level, the community was highly diverse, with a substantial proportion assigned to low-abundance or unclassified taxa. Besides *Escherichia–Shigella*, *Bacillus* and *Thermobifida* showed the clearest treatment-dependent responses (Fig. 4b). *Bacillus* was prominent in CK during the early stage; as a thermotolerant hydrolytic genus producing a broad range of extracellular enzymes, it contributes to protein degradation and organic-matter turnover (Jiang et al. 2024), and its prominence in CK is consistent with that treatment's moderate temperature regime.

Thermobifida showed the most pronounced amendment-specific response. This thermophilic actinomycete carries an efficient thermostable polysaccharide-hydrolase system and is frequently associated with cellulose degradation during composting (Bui et al. 2023). From the relative abundances in Online Resource 1, Table S1, *Thermobifida* reached 9.589% under $Na_2S_2O_8$ at day 5, against 0.385%, 0.214% and 0.217% in CK, Fe_3O_4 and MnO_2, approximately 24.9-fold higher than CK. Fe_3O_4 and MnO_2 in fact carried *Thermobifida* abundances slightly below CK; their leading position among identified genera in Fig. 4b reflects relative ranking within communities dominated by “others” rather than genuine enrichment, and should be read alongside Online Resource 1, Table S1. *Thermobifida* proliferation was therefore tied to the thermophilic conditions established by $Na_2S_2O_8$ rather than to amendment addition as such.

3.4 Amendment-specific association patterns

3.4.1 Physicochemical associations

Correlation analysis between physicochemical properties and humus-related components (Fig. 5) revealed a consistent humification gradient across all treatments. In every treatment, OM and the C/N ratio were positively correlated with HS, FA, and the protein-like component DOM-C1, but negatively correlated with the DP and the more humified components DOM-C2 and DOM-C3. Conversely, EC and TN were positively correlated with DP, DOM-C2, and DOM-C3. This pattern defines a transformation axis along which labile, OM- and C/N-rich fractions (FA, DOM-C1) are progressively converted into polymerized, humified fractions (DP, DOM-C2, DOM-C3) as composting proceeds, consistent with the

established view that humification entails the degradation of macromolecular precursors followed by their polymerization into humic substances.

The treatments differed most clearly in the variables accompanying HA formation. In CK, HS varied with FA ($r = 0.818$, $p = 0.025$) but not with HA ($r = 0.110$, $p = 0.81$), leaving the humic pool fulvic-dominated. Under $Na_2S_2O_8$, HA varied positively with the ·OH-equivalent ROS response ($r = 0.595$, $p = 0.16$), temperature, and pH, consistent with oxidative and thermal contributions to early HA formation but indicating a trend rather than a significant relationship across the seven time points. The only significant physicochemical association was EC with DP under Fe_3O_4 ($r = 0.848$, $p = 0.016$), positive in the same direction in the other three treatments ($r = 0.47$ to 0.73). The treatments therefore differ in the strength and timing of a shared transformation rather than in statistically distinguishable correlation structures.

3.4.2 Microbial associations

Phylum-level correlations with the humus-related components (Online Resource 1, Fig. S4) followed the same gradient. Planctomycetota, Acidobacteriota and Chloroflexi were positively associated with the less-humified fractions (FA, DOM-C1), whereas Actinobacteriota and Bacteroidota, joined by Firmicutes under $Na_2S_2O_8$, varied with HA, DP and the humic-like components. They agree with the established roles of Firmicutes and Bacteroidota in degrading lignocellulose and releasing humic precursors (Gharechahi et al. 2023; Huang et al. 2023).

3.5 Implications for returning sludge compost to land

Table 1 summarizes the attributes that govern how each compost can be returned to land. They fall into a pathogen-reduction dimension, set by the process thermal history, and a product-quality dimension, set by the humic composition, salinity, and elemental load of the finished compost; the amendments differed more clearly in the first than in the second.

Table 1
Process and product attributes relevant to returning the four composts to land

Attribute	CK	Fe_3O_4	MnO_2	$Na_2S_2O_8$
Peak temperature, °C (day)	44.2 (5)	47.5 (19)	46.0 (5)	68.0 (2)
Days at or above 50°C	0	0	0	6
Days at or above 55°C	0	0	0	4
United States condition met (≥ 55°C, 3 days)[a]	No	No	No	Yes
Chinese guideline met (≥ 55°C, 6 days)[a]	No	No	No	No (4 of 6 days)
Escherichia–Shigella, day 5 (%)	5.76	13.40	6.03	0.10
Escherichia–Shigella, day 42 (%)	0.13	0.09	0.08	0.14
Organic-matter degradation (%)	49.95 ± 2.77	55.53 ± 1.21	52.19 ± 0.49	56.53 ± 0.42
Humic acid, day 42 (mg g^{-1})	27.22 ± 0.07	29.06 ± 0.10	29.38 ± 0.47	29.50 ± 0.30
Degree of polymerization, day 42	1.23 ± 0.005	1.27 ± 0.007	1.29 ± 0.022	1.33 ± 0.006
Total humic substances, day 42 (mg g^{-1})	53.75 ± 0.02	55.75 ± 0.10	59.34 ± 0.91	58.65 ± 0.02
Change in total humic substances from day 0 (%)	−24.3	−21.8	−16.7	−18.7
Final EC (mS cm^{-1})	1.98	2.06	2.05	3.00
Final pH	8.75	7.65	7.52	7.32
Final C/N	11.20	11.18	11.63	10.12
Element added (g kg^{-1} dry feedstock)[b]	–	Fe 7.2	Mn 6.3	Na 1.9; S 2.7

[a] Time–temperature conditions for in-vessel composting of sewage sludge (US EPA 1993) and for sludge aerobic fermentation (Ministry of Housing and Urban-Rural Development 2011); durations were measured in 60 L reactors. [b] Calculated from the 1% (w/w) dose and the amendment stoichiometry. Other values are means ± standard deviation (n = 3) or treatment means.

$Na_2S_2O_8$ was the only amendment to produce a thermophilic cycle at this dose, reaching 68°C and holding above 50°C for six consecutive days. It was also the only treatment to meet a recognized time–temperature condition for pathogen reduction in sludge and to prevent the early regrowth of *Escherichia–*

Shigella. It gave the highest DP (1.33), the fastest early HA accumulation (31.49 mg g^{-1} by day 5), and the greatest organic-matter degradation (56.53%). Where the compost must satisfy a time–temperature pathogen-reduction requirement before land application and the feedstock cannot reach it unaided, it was the only one of the three to do so. A second consideration is the elevated ionic load: EC rose to 3.00 mS cm^{-1} against 1.98 mS cm^{-1} in CK, which warrants consideration for salinity-sensitive end uses. Together with the 1.9 g Na and 2.7 g S added per kg of dry feedstock, this load should match the salt tolerance of the receiving soil and crop.

MnO_2 retained as much total humic substance at day 42 as $Na_2S_2O_8$ (59.34 and 58.65 mg g^{-1}, against 53.75 mg g^{-1} in CK; $p = 0.001$ for MnO_2 against CK), although its final HA content was close to that of the other two amendments, and it introduced no additional salinity. Where humic content matters and pathogen reduction is achieved by other means, MnO_2 offers comparable humic retention without added salinity, but it adds 6.3 g Mn per kg of dry feedstock, a load that should be judged against the receiving soil. Fe_3O_4 gives intermediate results: a DP of 1.27, the slowest thermal profile apart from its late self-heating episode, and the lowest total HS of the three amendments (55.75 mg g^{-1}), and it amplified the early regrowth of *Escherichia–Shigella*; its distinguishing feature is the association of humification indicators with EC rather than with the oxidative peak.

Two limitations bound these comparisons. (1) The fate of residual Fe, Mn, and sulfate in the product, and their behavior after land application, was not examined. (2) No agronomic testing was performed, so the practical value of a 0.04 to 0.10 rise in DP relative to the control remains to be established. Technical or industrial grades would also replace the reagent-grade materials used here at operating scale. A further implication concerns how the recycled product is certified. The degree of polymerization rose in every treatment while total humic substances fell by 17 to 24%, so a maturity criterion based on humic ratios alone would certify all four composts as more humified, even as the humic carbon they return to soil declined. Where compost is certified for land application, ratio-based indices should be paired with an absolute measure of humic or organic carbon.

4. Conclusions

Under identical feedstock, dose, and duration, Fe_3O_4, MnO_2, and $Na_2S_2O_8$ did not act interchangeably. Only $Na_2S_2O_8$ produced a thermophilic cycle, reaching 68°C and staying above 50°C for six consecutive days; it was also the only treatment to meet a recognized time–temperature condition for pathogen reduction in sludge and to prevent the early regrowth of *Escherichia–Shigella*, and it gave the highest degree of polymerization and the greatest organic-matter degradation. The persulfate-driven thermophilic phase also selected a distinct bacterial community, enriched in Firmicutes, Actinobacteriota, and the cellulose-degrading *Thermobifida*, whereas the metal oxides favored Proteobacteria and Bacteroidota, and Fe_3O_4 more than doubled the early *Escherichia–Shigella* bloom. MnO_2 retained as much humic substance as $Na_2S_2O_8$ without added salinity but never crossed the thermophilic threshold, and Fe_3O_4 gave intermediate values with a delayed self-heating episode late in

composting. Amendment choice therefore determines which product property improves, and is a process decision rather than a uniform enhancement of humification.

The comparison also shows that humification indices and humic quantity can move in opposite directions. The degree of polymerization rose in every treatment. At the same time, total humic substances fell by 17 to 24%, so ratio-based maturity indices can indicate progressive humification in a system that is losing humic carbon and should be read alongside an absolute measurement whenever compost is certified for land application. Both findings point in the same direction: specify the compost's intended use before choosing either the amendment or the maturity criterion. For sludge whose C/N ratio is too low to sustain self-heating, chemical amendment offers a route to a thermophilic cycle that meets a recognized pathogen-reduction condition, without altering the bulking-agent recipe; where the product's humic content matters more than cycle speed, a different amendment and a different measure of maturity apply.

Declarations

Competing interests:

The authors have no relevant financial or non-financial interests to disclose.

Ethics approval:

Not applicable.

Funding:

This study was funded by the Natural Science Foundation of Guangdong Province (2024A1515010980) and the National Natural Science Foundation of China (42477225).

Author Contribution

Meihua Zhao: Writing – review & editing, Funding acquisition, Project administration. Zhiyu Cen: Writing – original draft, Methodology, Formal analysis, Data curation, Visualization. Zhen Yu: Writing – review & editing, Conceptualization, Validation. Sirui Xu: Methodology, Visualization. François Nkinahamira: Writing – review & editing, Supervision, Software.

Data Availability

The datasets generated and analyzed during the current study are available from the corresponding author on reasonable request

References

1. Balkrishna A, Banerjee S, Ghosh S, et al (2024) Reuse of sewage sludge as organic agricultural products: An efficient technology-based initiative. Appl Environ Soil Sci 2024:1433973. https://doi.org/10.1155/2024/1433973
2. Bang D, Chung W, Chang S (2024) Influence of effective microbial additives inoculation on indigenous bacterial community dynamics and co-occurrence patterns during the composting of mixed food waste and livestock manure. Agronomy 14:2973. https://doi.org/10.3390/agronomy14122973
3. Bui VKH, Truong HB, Hong S, et al (2023) Biotic and abiotic catalysts for enhanced humification in composting: A comprehensive review. J Clean Prod 402:136832. https://doi.org/10.1016/j.jclepro.2023.136832
4. Chen L, Chen Y, Li Y, et al (2023) Improving the humification by additives during composting: A review. Waste Manag 158:93–106. https://doi.org/10.1016/j.wasman.2022.12.040
5. Chen L, Zhang Z, Yang R, et al (2024) Nano Fe_3O_4 improved the electron donating capacity of dissolved organic matter during sludge composting. J Environ Manage 369:122354. https://doi.org/10.1016/j.jenvman.2024.122354
6. Feng J, Burke IT, Chen X, Stewart DI (2023) Assessing metal contamination and speciation in sewage sludge: implications for soil application and environmental risk. Rev Environ Sci Biotechnol 22:1037–1058. https://doi.org/10.1007/s11157-023-09675-y
7. Gharechahi J, Vahidi MF, Sharifi G, et al (2023) Lignocellulose degradation by rumen bacterial communities: New insights from metagenome analyses. Environ Res 229:115925. https://doi.org/10.1016/j.envres.2023.115925
8. Guo X, Liu H, Wu S (2019) Humic substances developed during organic waste composting: Formation mechanisms, structural properties, and agronomic functions. Sci Total Environ 662:501–510. https://doi.org/10.1016/j.scitotenv.2019.01.137
9. Hamoda MF, Abu Qdais HA, Newham J (1998) Evaluation of municipal solid waste composting kinetics. Resour Conserv Recycl 23:209–223. https://doi.org/10.1016/S0921-3449(98)00021-4
10. Hong W, Zou J, Zhao M, et al (2024) Development of a five-chemical-probe method to determine multiple radicals simultaneously in hydroxyl and sulfate radical-mediated advanced oxidation processes. Environ Sci Technol 58:5616–5626. https://doi.org/10.1021/acs.est.4c00669
11. Huang J, Gao K, Yang L, Lu Y (2023) Successional action of Bacteroidota and Firmicutes in decomposing straw polymers in a paddy soil. Environ Microbiome 18:76. https://doi.org/10.1186/s40793-023-00533-6
12. Jiang J, Cui H, Tang Z, et al (2024) Synergistic effects of biochar and laccase on nitrogen conversation and degradations of two artificial sweeteners during the sewage sludge composting. Chem Eng J 498:155732. https://doi.org/10.1016/j.cej.2024.155732

13. Li H, Yang Z, Zhang C, et al (2024) Effect of microbial inoculum on composting efficiency in the composting process of spent mushroom substrate and chicken manure. J Environ Manage 353:120145. https://doi.org/10.1016/j.jenvman.2024.120145
14. Li L, Hua Y, Zhao S, et al (2023) Worldwide research progress and trend in sludge treatment and disposal: A bibliometric analysis. ACS ES&T Eng 3:1083–1097. https://doi.org/10.1021/acsestengg.3c00149
15. Liu X, Yu Z, Zhao M, et al (2026) Governing the fate of heavy metals: A review on complexation with compost-derived dissolved organic matter. J Environ Manage 403:129252. https://doi.org/10.1016/j.jenvman.2026.129252
16. Liu Y, Zhou J, Lu S, Ren J (2025) Towards the new era of sewage sludge management in China: Status, challenges, and perspectives. Process Saf Environ Prot 198:107201. https://doi.org/10.1016/j.psep.2025.107201
17. Lu M, Hao Y, Lin B, et al (2024) The bioaugmentation effect of microbial inoculants on humic acid formation during co-composting of bagasse and cow manure. Environ Res 252:118604. https://doi.org/10.1016/j.envres.2024.118604
18. Lu X, Liu H-B, Li Q (2025) Reactive oxygen species act efficiently as catalysts in novel composting humification pathways. J Environ Chem Eng 13:117198. https://doi.org/10.1016/j.jece.2025.117198
19. Luo Z, Wang C, Sánchez-Montes I, Gamal El-Din M (2026) A one-step strategy for Cu(II)-EDTA decomplexation and copper precipitation via microwave-alkaline synergistic activation of persulfate. J Environ Chem Eng 14:123622. https://doi.org/10.1016/j.jece.2026.123622
20. Ministry of Environmental Protection of China (2012) Water quality: Determination of total nitrogen, alkaline potassium persulfate digestion UV spectrophotometric method (HJ 636–2012, in Chinese). China Environmental Science Press, Beijing
21. Ministry of Housing and Urban-Rural Development (2011) Technical guideline for treatment and disposal of sludge from municipal wastewater treatment plants (trial) (Jianke [2011] No. 34, issued with the National Development and Reform Commission, in Chinese). https://www.mohurd.gov.cn/gongkai/zhengce/zhengcefilelib/201103/20110330_203014.html. Accessed 1 Oct 2026
22. Nkinahamira F, Suanon F, Chi Q, et al (2019) Occurrence, geochemical fractionation, and environmental risk assessment of major and trace elements in sewage sludge. J Environ Manage 249:109427. https://doi.org/10.1016/j.jenvman.2019.109427
23. Pan T, Zhou Y-Y, Xiang Q, et al (2024) Efficient elimination of antibiotics and antibiotic resistance genes in hyperthermophilic sludge composting. J Hazard Mater 479:135525. https://doi.org/10.1016/j.jhazmat.2024.135525
24. Paredes C, Roig A, Bernal MP, et al (2000) Evolution of organic matter and nitrogen during co-composting of olive mill wastewater with solid organic wastes. Biol Fertil Soils 32:222–227. https://doi.org/10.1007/s003740000239

25. Puyuelo B, Ponsá S, Gea T, Sánchez A (2011) Determining C/N ratios for typical organic wastes using biodegradable fractions. Chemosphere 85:653–659. https://doi.org/10.1016/j.chemosphere.2011.07.014
26. Qi H, Gao W, Xie L, et al (2024) Effect of MnO_2-biochar composites on promoting humification during chicken manure composting. Biochar 6:32. https://doi.org/10.1007/s42773-024-00315-4
27. Qi H, Zhao Y, Wang X, et al (2021) Manganese dioxide driven the carbon and nitrogen transformation by activating the complementary effects of core bacteria in composting. Bioresour Technol 330:124960. https://doi.org/10.1016/j.biortech.2021.124960
28. Shen B, Zheng L, Zheng X, et al (2024) Insights from meta-analysis on carbon to nitrogen ratios in aerobic composting of agricultural residues. Bioresour Technol 413:131416. https://doi.org/10.1016/j.biortech.2024.131416
29. Ste-Marie L, Boismenu D, Vachon L, Montgomery J (1996) Evaluation of sodium 4-hydroxybenzoate as an hydroxyl radical trap using gas chromatography–mass spectrometry and high-performance liquid chromatography with electrochemical detection. Anal Biochem 241:67–74. https://doi.org/10.1006/abio.1996.0379
30. Sun X, Awasthi MK (2025) Synergistic effect and mechanism analysis of biochar regulator on heavy metal passivation and microplastic degradation in sewage sludge compost. J Hazard Mater 494:138551. https://doi.org/10.1016/j.jhazmat.2025.138551
31. Tao W, Deng Y, Li K, et al (2025) Mechanistic insights into humic acid formation from lignocellulosic waste via aerobic composting: A review. Int J Biol Macromol 330:148283. https://doi.org/10.1016/j.ijbiomac.2025.148283
32. US EPA (1993) Standards for the use or disposal of sewage sludge, 40 CFR Part 503, Appendix B: Pathogen treatment processes. In: United States Environmental Protection Agency. https://www.ecfr.gov/current/title-40/chapter-I/subchapter-O/part-503/appendix-Appendix%20B%20to%20Part%20503. Accessed 1 Oct 2026
33. Wang F, Zhou F, Zhang L, et al (2025) Mechanisms of manganese-modified biochar and white-rot fungi in enhancing compost humification: Boosting polyphenol pathway by lignocellulose degradation. Chem Eng J 507:160637. https://doi.org/10.1016/j.cej.2025.160637
34. Wang K, Zhang M, Chen C, et al (2026) Sodium persulfate/manganese dioxide/ferrous sulfate synergistically enhance the ability of functional microorganisms to accelerate humification during composting. Environ Technol 47:741–754. https://doi.org/10.1080/09593330.2025.2601334
35. Wang S, Meng Q, Zhu Q, et al (2021) Efficient decomposition of lignocellulose and improved composting performances driven by thermally activated persulfate based on metagenomics analysis. Sci Total Environ 794:148530. https://doi.org/10.1016/j.scitotenv.2021.148530
36. Xie T, Zhang Z, Yu Y, et al (2023) Aeration intensity drives dissolved organic matter transformation and humification during composting by regulating the organics metabolic functions of microbiome. Chem Eng J 476:146645. https://doi.org/10.1016/j.cej.2023.146645

37. Xing R, Chen Z, Sun H, et al (2022) Free radicals accelerate in situ ageing of microplastics during sludge composting. J Hazard Mater 429:128405. https://doi.org/10.1016/j.jhazmat.2022.128405
38. Yang S-Q, Cui Y-H, Li J-Y, et al (2020) Determination methods for steady-state concentrations of HO• and $SO_4^{\bullet -}$ in electrochemical advanced oxidation processes. Chemosphere 261:127658. https://doi.org/10.1016/j.chemosphere.2020.127658
39. Zhao M, Zhou X, Cai W, Nkinahamira F (2026) Engineering sustainable compost synthesis via divergent mechanistic pathways of plant- and animal-derived biochars for nitrogen valorization. Sustain Chem Pharm 50:102335. https://doi.org/10.1016/j.scp.2026.102335
40. Zhou X, Yu Z, Deng W, et al (2024) Hyperthermophilic composting coupled with vermicomposting stimulates transformation of organic matter by altering bacterial community. Sci Total Environ 954:176676. https://doi.org/10.1016/j.scitotenv.2024.176676

Figures

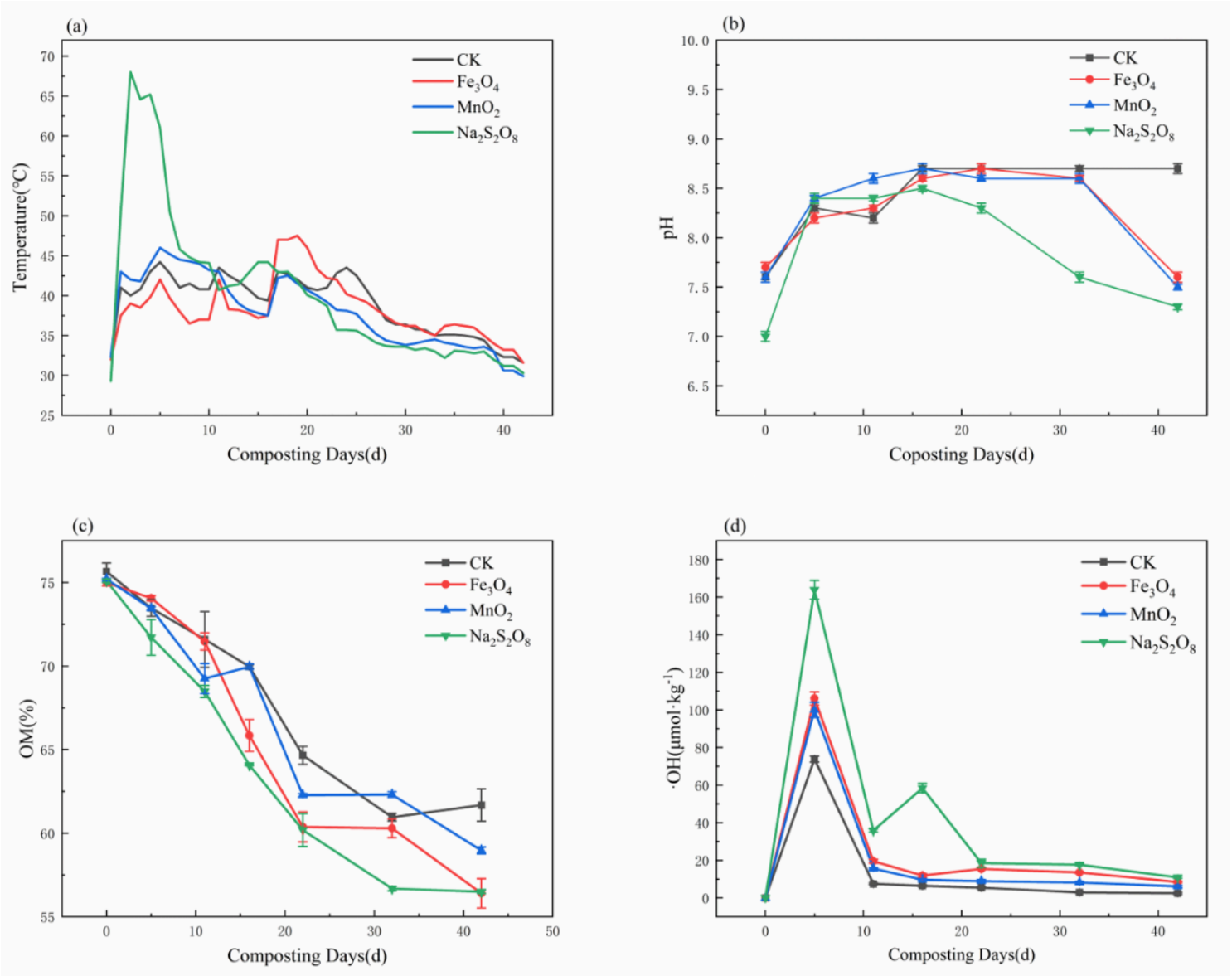


Figure 1

Evolution of physicochemical properties during 42-day composting of sewage sludge under control (CK) and Fe_3O_4, MnO_2, and $Na_2S_2O_8$ amendments: (a) temperature (°C); (b) pH; (c) organic matter content (%); and (d) ·OH-equivalent reactive oxygen species concentration (μmol kg^{-1}). Values are means ± standard deviation (n = 3)

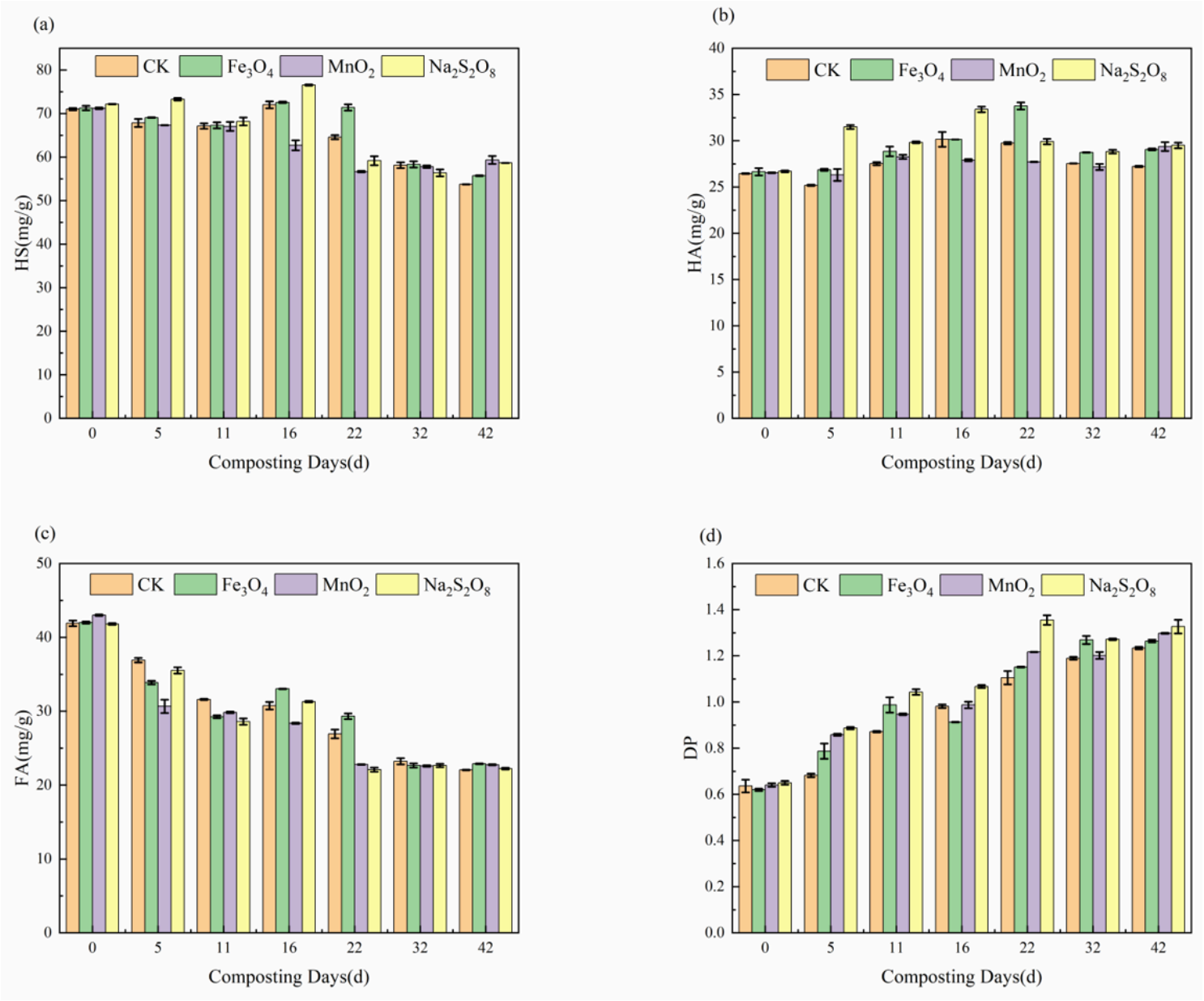


Figure 2

Evolution of humic fractions during 42-day composting of sewage sludge under control (CK) and Fe_3O_4, MnO_2, and $Na_2S_2O_8$ treatments: (a) humic substances (HS, mg g^{-1}); (b) humic acid (HA, mg g^{-1}); (c) fulvic acid (FA, mg g^{-1}); and (d) degree of polymerization (DP = HA/FA). Values are means ± standard deviation (n = 3)

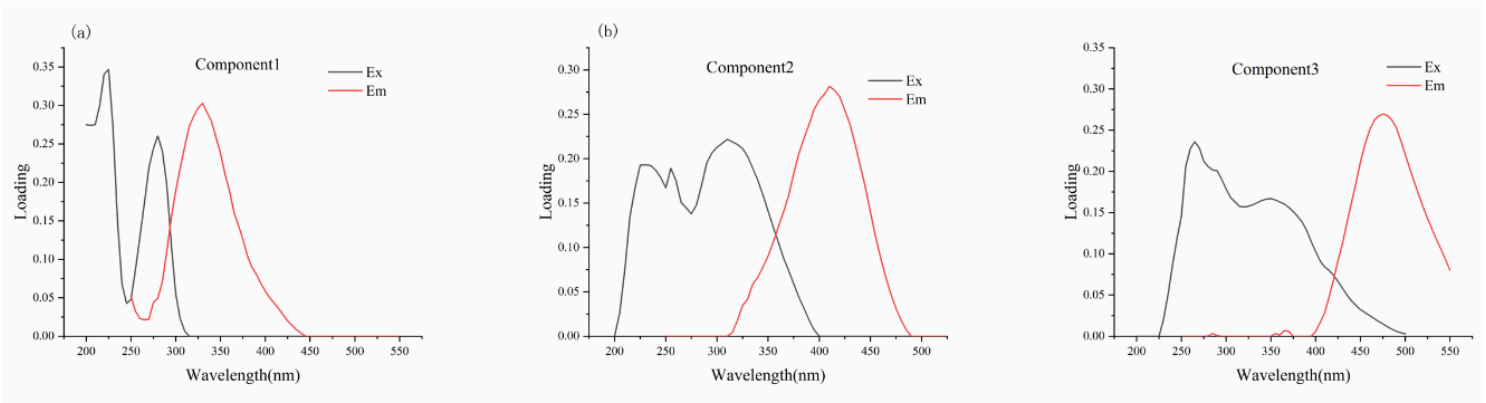


Figure 3

Excitation (black) and emission (red) loading spectra of the three fluorescent components resolved by EEM-PARAFAC: (a) C1, protein-like (Ex/Em 225–280/330 and 300–350/400 nm); (b) C2, humic acid-like (Ex/Em 230–255/410 nm); and (c) C3, highly conjugated humic-like (Em ≈ 475 nm)

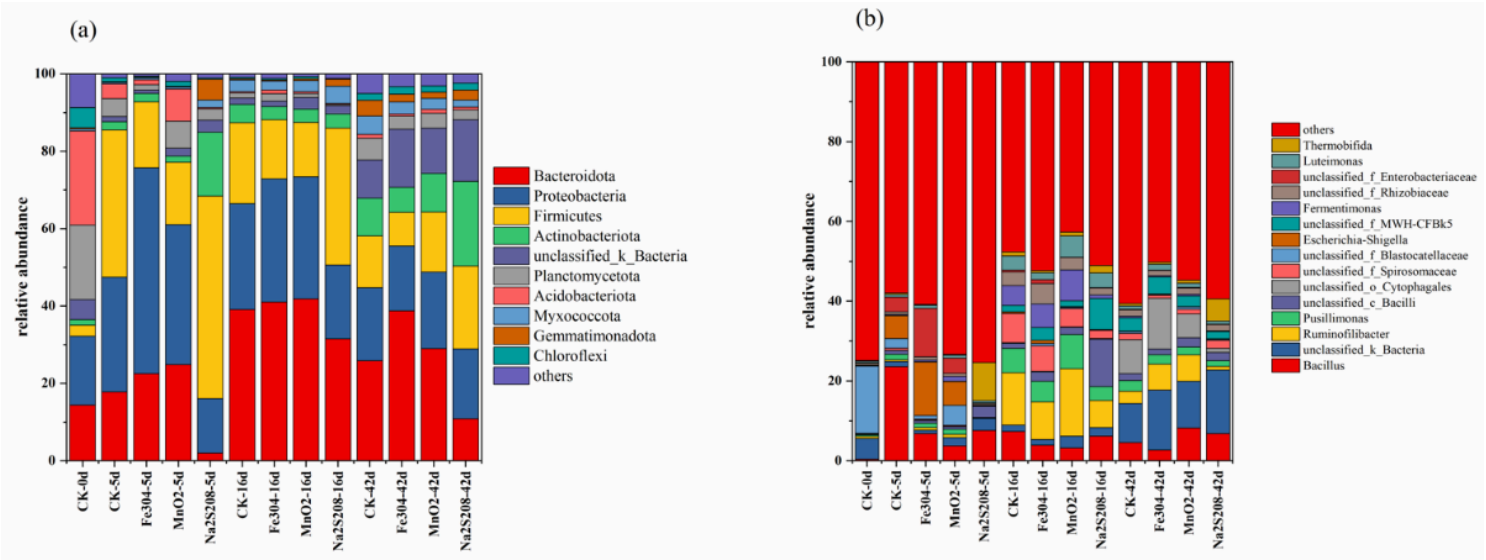


Figure 4

Bacterial community succession during 42-day composting of sewage sludge under control (CK) and Fe_3O_4, MnO_2, and $Na_2S_2O_8$ treatments, based on 16S rRNA gene sequencing: (a) relative abundance at the phylum level; (b) relative abundance at the genus level

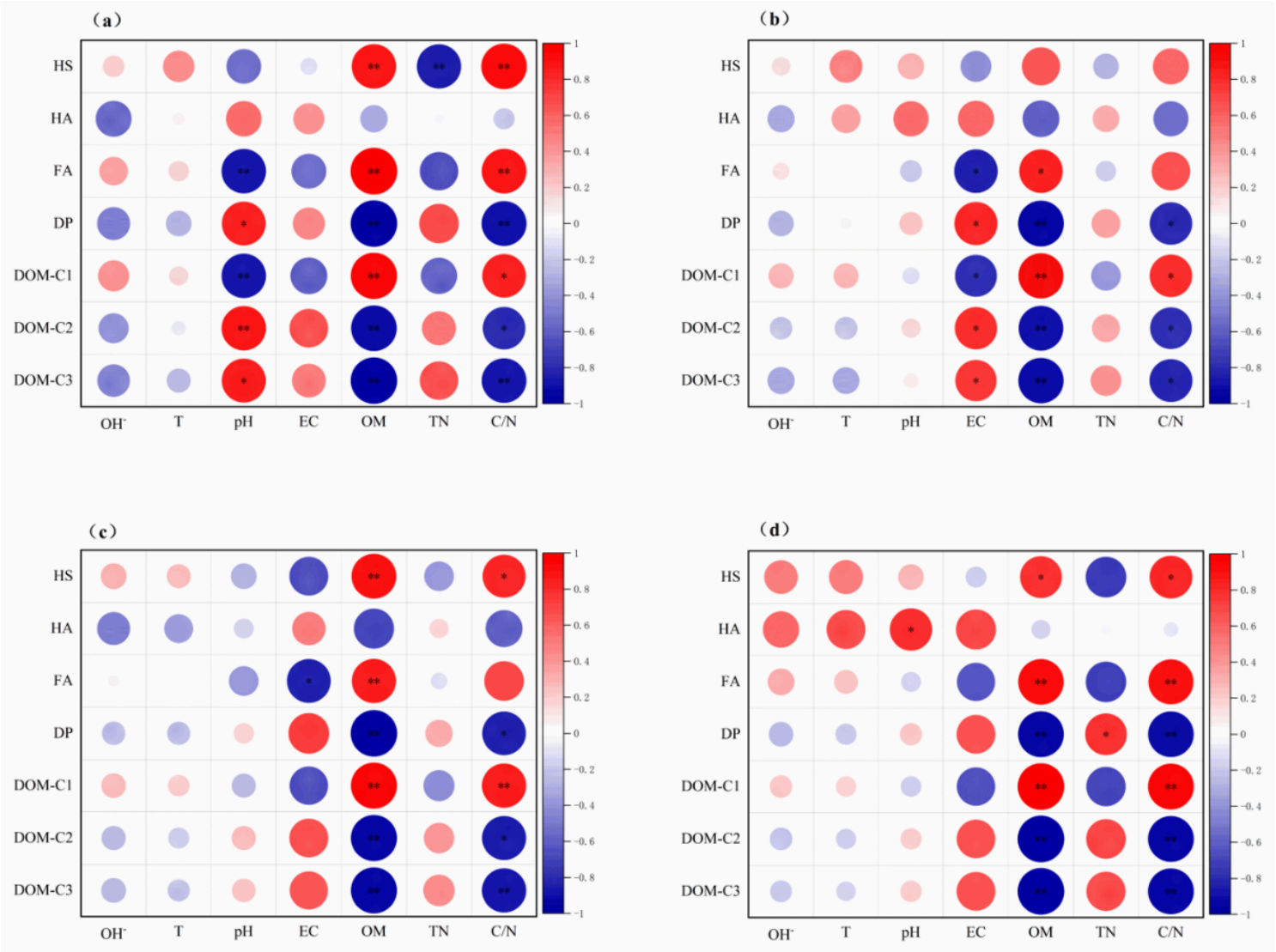


Figure 5

Correlations between physicochemical properties and humus-related components (HS, HA, FA, DP, DOM-C1–C3) under control (CK), Fe_3O_4, MnO_2, and $Na_2S_2O_8$ treatments. Color and circle size indicate correlation direction and strength; asterisks indicate significance. Coefficients were calculated from treatment means at seven sampling points (n = 7); at this sample size, $p < 0.05$ and $p < 0.01$ require $|r| > 0.754$ and $|r| > 0.875$, respectively

Supplementary Files

This is a list of supplementary files associated with this preprint. Click to download.

- ManuscriptBiodegradationclean.docx